DOI: 10.1002/ange.201306673

Heterogeneous Catalysis

Following Solid-Acid-Catalyzed Reactions by MAS NMR Spectroscopy in Liquid Phase—Zeolite-Catalyzed Conversion of Cyclohexanol in Water**

*Aleksei Vjunov, Mary Y. Hu, Ju Feng, Donald M. Camaioni, Donghai Mei, Jian Z. Hu, Chen Zhao, and Johannes A. Lercher**

Abstract: *A microautoclave magic angle spinning NMR rotor is developed enabling in situ monitoring of solid–liquid–gas reactions at high temperatures and pressures. It is used in a kinetic and mechanistic study of the reactions of cyclohexanol on zeolite HBEA in 130°C water. The ^{13}C spectra show that dehydration of 1-^{13}C-cyclohexanol occurs with significant migration of the hydroxy group in cyclohexanol and the double bond in cyclohexene with respect to the ^{13}C label. A simplified kinetic model shows the E1-type elimination fully accounts for the initial rates of 1-^{13}C-cyclohexanol disappearance and the appearance of the differently labeled products, thus suggesting that the cyclohexyl cation undergoes a 1,2-hydride shift competitive with rehydration and deprotonation. Concurrent with the dehydration, trace amounts of dicyclohexyl ether are observed, and in approaching equilibrium, a secondary product, cyclohexyl-1-cyclohexene is formed. Compared to phosphoric acid, HBEA is shown to be a more active catalyst exhibiting a dehydration rate that is 100-fold faster per proton.*

The efficient catalytic hydrodeoxygenation (HDO) of phenols over metals, such as Pt,[1] Pd,[2] or Ni,[3] requires an acid function to catalyze dehydration of the intermediately formed cycloalkanols. Surprisingly, the rate of dehydration normalized to the concentration of protons is about two orders of magnitude higher in a zeolite than in aqueous solution of a mineral acid.[4] It is also remarkable that hydroalkylation of phenol on zeolite HBEA can occur in water, while other macroporous solid acids do not catalyze this reaction.[1,5] It can be speculated that zeolites achieve this by providing an environment (sometimes called confinement and nest effects),[6] which uniquely stabilizes the sorbed and transition states.[7] To better understand the catalysis we have undertaken substantial efforts to monitor the state of the reacting molecules by spectroscopic methods. The information obtained potentially allows one not only to understand the mechanistic pathways, but provides also the basis to design new and improve existing zeolites with respect to activity and selectivity.

The dehydration of secondary alcohols in aqueous phase catalyzed by mineral acids generally proceeds by the E1 mechanism.[8] Also, alcohol dehydration in the gas phase using polyoxometalate[9] and zeolite[10] catalysts has been suggested to follow strictly the E1 elimination pathway. The catalyst acidity determined by the zeolite lattice composition[7] and the pore size[11] jointly control activity and selectivity for catalytic gas phase reactions. Herein we elucidate the mechanism of the reaction of aqueous cyclohexanol on zeolite HBEA by magic angle spinning (MAS) nuclear magnetic resonance (NMR) spectroscopy, which enables simultaneous monitoring of the state of reactants, intermediates, and products, thereby providing mechanistic insight through following the variations in isotopomer concentrations during catalytic transformations.

While in situ MAS-NMR spectroscopy has been developed to study gas–solid reactions in controlled environments,[12] following reactions in liquid phase during the formation of solids was the limit for studying reactions during the synthesis of zeolites.[13] It has not been possible, to date, to monitor two- and three-phase reactions involving solids, gases, and liquids at elevated temperatures and pressures.[14] To address this we have constructed a microautoclave that functions as MAS-NMR rotor and allows batch reactions with pressures of up to 20 bar independent of the gas atmosphere and temperatures of up to 200°C, thus allowing mechanistic studies of most reactions in organic synthesis. The detailed design of the microautoclave that can be repeatedly sealed is illustrated in Figure 1. The rotor can withstand spinning the sample at elevated temperature and pressure with the design yielding negligible ^{13}C background signal (see the Supporting Information for detail). The reactor

[*] A. Vjunov, M. Y. Hu, Dr. J. Feng, Dr. D. M. Camaioni, Dr. D. Mei, Dr. J. Z. Hu, Prof. Dr. J. A. Lercher
Institute for Integrated Catalysis
Pacific Northwest National Laboratory
P.O. Box 999, Richland, WA 99352 (USA)
E-mail: johannes.lercher@pnnl.gov
Dr. C. Zhao, Prof. Dr. J. A. Lercher
Department of Chemistry and Catalysis Research Institute
TU München
Lichtenbergstrasse 4, 85748 Garching (Germany)

[**] We thank Zizwe A. Chase and Junming Sun (both from Washington State University) for pretreating the catalyst. C.F. Peden is acknowledged for his support in developing the NMR capability. This work was supported by the U. S. Department of Energy (DOE), Office of Basic Energy Sciences, Division of Chemical Sciences, Geosciences & Biosciences. All experiments were performed at the Environmental Molecular Sciences Laboratory, a national scientific user facility sponsored by the DOE's Office of Biological and Environmental Research located at Pacific Northwest National Laboratory (PNNL). PNNL is a multiprogram national laboratory operated for DOE by Battelle Memorial Institute under Contract no. DE-AC06-76L0-1830.

Supporting information for this article is available on the WWW under http://dx.doi.org/10.1002/anie.201306673.

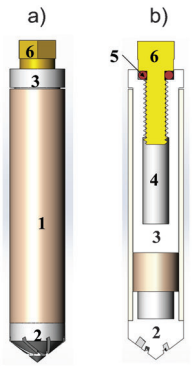

Figure 1. The 9.5 mm outer diameter high-temperature and high-pressure MAS rotor is shown. a) The fully assembled rotor; and b) the various components, i.e., the zirconia rotor sleeve (1), the ceramic insert made of materials such as Macor (2), the sample cell space (3) and thread (4), O ring (5), and Torlon screw (6). The outside surface of the insert is fixed to the inner surface of the zirconia rotor sleeve by high-temperature glue.

is also suitable for operation with exogeneous high-pressure gas using a loading chamber that allows sealing and opening of the rotor in a controlled atmosphere.[15] The lid of the microautoclave and the valve adaptor to pressurize it, are removable. Thus, operation at pressures exceeding 20 bar is possible with marginal gas leaking for up to 72 h.

Let us now turn to a typical experiment using a solid catalyst, i.e., HBEA150 zeolite (about 25 mg for a typical example) and 125 μL of 0.33 M 1-^{13}C-cyclohexanol in water. The catalyst and the reactants were sealed in the rotor, while NMR data were acquired at an estimated reaction temperature of 130 °C, as function of time. After 23 h this led to 36 % cyclohexene, 3 % dicyclohexyl ether, and 1 % cyclohexyl-1-cyclohexene. The forward rate constant for cyclohexene formation was $k_f = 3.4 \times 10^{-5}\ s^{-1}$ (see the Supporting Information for detail); the turnover frequency (TOF) was determined as the initial forward rate normalized by the concentration of Brønsted acid sites, $TOF = 4.2 \times 10^{-4}\ mol_{cyclohexene}\, mol_{BAS}^{-1}\, s^{-1}$.

Figure 2 shows the series of NMR spectra following the conversion of cyclohexanol and an example for a single spectrum with the assignment of individual ^{13}C signals. Initially 1-^{13}C-cyclohexanol is observed as a narrow peak at about 70 ppm, corresponding to 1-^{13}C-cyclohexanol in the aqueous phase, and a broad peak at about 70.8 ppm, which is attributed to 1-^{13}C-cyclohexanol interacting with the zeolite. Using these two peaks we estimate that about 50 % of the cyclohexanol present is initially adsorbed in the zeolite pores.

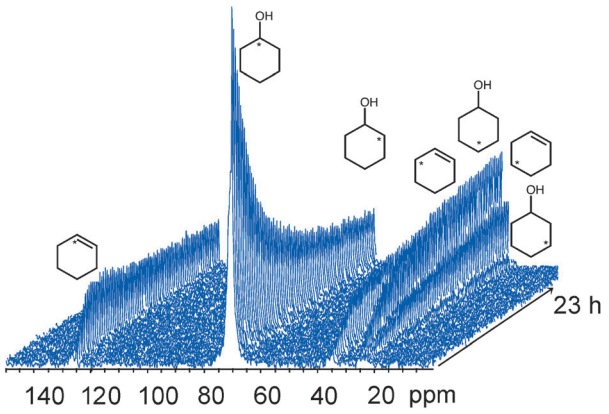

Figure 2. Stacked plot containing 80 MAS-NMR spectra acquired for a mixture of 22 mg HBEA150 and 120 μL of 0.33 M 1-^{13}C-cyclohexanol at 130 °C in liquid water and as a function of time.

A nearly identical value is observed for cyclohexene, thus suggesting that the dispersion forces account for the largest fraction of the interaction energy.[16] Note that water fills the zeolite pores, while cyclohexanol occupies only up to 25 % of the pore volume during the reaction. Nevertheless this corresponds to a significant (20-fold) enhancement of the concentration of cyclohexanol compared to the aqueous phase. This exemplifies the potential to determine not only changes in concentrations, but also how it is possible to quantify the distribution between the adsorbed and the mobile phase at elevated pressures and temperatures.

At the start of the reaction, formation of cyclohexene and dicyclohexyl ether is observed together with scrambling of the ^{13}C label in the alicyclic ring. As the reaction progresses a secondary product, cyclohexyl-1-cyclohexene, is detected. At long reaction time quantification of products appearing in low concentration is hindered by the diversity of labeled products and long spin lattice relation times ($T1$) for the carbon atoms without attached hydrogen atoms. However, ≥ 96 % of the ^{13}C could be accounted for as cyclohexanol and cyclohexene during the initial reaction stage (2 h); the slight signal loss is attributed to low initial concentrations of dicyclohexyl ether and cyclohexyl-1-cyclohexene that would require a higher signal-to-noise ratio to measure accurately.

To determine which mechanism, E1 or E2, operates in the dehydration of cyclohexanol, the ^{13}C-label scrambling was analyzed and the initial rates of disappearance of 1-^{13}C-cyclohexanol and the appearance of the differently labeled products were determined. A simplified kinetic model (see the Supporting Information) shows the E1-type elimination via carbenium ions fully accounting for all initial rates, suggesting that the cyclohexyl cation undergoes a 1,2-hydride shift competitive with rehydration and deprotonation.[17] The model shows that the rate of the 1,2-hydride shift approximately equals that of deprotonation and is approximately half the rate of the rehydration of cyclohexene (Figure S7 in the Supporting Information). As dehydration approaches equilibrium, the probability for an electrophilic attack of a cyclohexyl carbenium ion on cyclohexene to form cyclohexyl-1-cyclohexene increases. The cyclohexyl cation is concluded to be the central intermediate, which explains the reaction products, as well as the rapid migration of the hydroxy group and double bond away from the ^{13}C-labeled carbon. An E2-type elimination kinetic model cannot account for these rates. The mechanism determined by virtue of in situ NMR analysis and proposed herein is shown in Scheme 1.

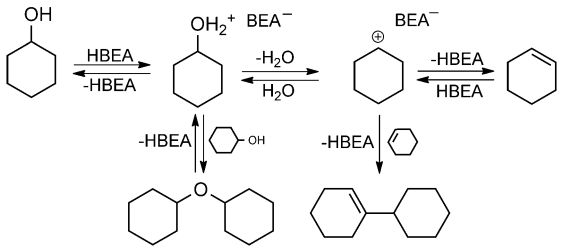

Scheme 1. Proposed reaction pathway of cyclohexanol reacting in liquid water on HBEA.

In the absence of water, alcohol dehydration on zeolites has been suggested to proceed through the E1-mechanistic pathway,[18] with the formation of surface-bound alkoxide species and water constituting the rate-determining step.[19] In contrast, a corresponding species was not observed in MAS-NMR (zeolite$^+$-O$^-$R) in presence of larger concentrations of liquid water. In passing it should also be mentioned that such alkoxides have been suggested to be unstable even in the presence of gaseous water.[20]

The E2 mechanism, requiring the C–O and β C–H bonds to be cleaved concertedly, is not relevant in the present case. If this pathway were dominant, then the initial rate of disappearance of the starting 1-^{13}C-cyclohexanol should equal the initial rate of appearance of cyclohexene. Since this step is reversible, the ^{13}C scrambling would be explained by hydration of cyclohexene leading to equal probability for the label to be in either the 1- or 2-labeled position of cyclohexanol. However, the initial rate for disappearance of 1-^{13}C-cyclohexanol is 2.5 times the initial rate of formation of 1-^{13}C-cyclohexene. Furthermore, the initial rates for formation of 2-^{13}C-cyclohexanol and 3-^{13}C-cyclohexene are 0.2 and 0.1 times the initial rate of disappearance of 1-^{13}C-cyclohexanol, respectively. Thus, on basis of these individual rates an E2-type elimination mechanism can be excluded.

Given that hydronium ions or Brønsted acid sites are the catalytically active species, it is important to compare the specific catalytic activity of Brønsted acid sites (BAS) in zeolites with the activity of hydronium ions in acidic aqueous solutions. The comparison of the reactivity of zeolite HBEA with that of phosphoric acid at 160 °C shows under identical reaction conditions a TOF value of $1.0\times10^{-2}\,mol_{cyclohexene}\,mol_{BAS}^{-1}\,s^{-1}$ for the zeolite and $1.4\times10^{-4}\,mol_{cyclohexene}\,mol_{BAS}^{-1}\,s^{-1}$ for H_3PO_4, i.e., the zeolite has over a 100 times higher turnover frequency (see the Supporting Information for details). Because the dehydration displays a first-order dependence in cyclohexanol for the zeolite as well as the mineral acid, it is concluded that the concentration of acid sites that interact with cyclohexanol must be low. This raises the question, why the rate is substantially higher in the case of the zeolite. While the presence of sufficient water leads to hydronium ions in both cases, the environment of the zeolite pore is shown to stabilize the transition state such that the activation entropy for the dehydration is significantly higher in the case of the zeolite.[21] A further interpretation is beyond the scope of the present contribution. Note, that preliminary results of theoretical calculations indeed point to a stabilization of the hydroxonium ion transition state.

Because C–C coupling products are observed in the presence of zeolite, but not when catalyzed by aqueous H_3PO_4, we conclude that also in this case the zeolite pores exert a specific influence stabilizing the transition state of the bimolecular reaction.[19]

These reaction pathways are in line with computational modeling in the absence of water indicating that cyclohexanol adsorbs on Brønsted acid sites with a binding energy of 116 kJ mol^{-1}, which is significantly higher than the binding energy of water (45 kJ mol^{-1}). Cyclohexanol is spontaneously protonated upon adsorption, with proton transfer being thermodynamically favored by 29 kJ mol^{-1}. Calculation shows that decomposition of the protonated cyclohexanol into cyclohexyl cation and water through C–O bond scission is an endothermic step and rate limiting with an activation barrier of 97 kJ mol^{-1}. After C–O bond scission a β-methylene proton of the cyclohexyl cation is transferred back to HBEA, thereby reforming the zeolite hydroxy group and leading to cyclohexene, which is favored over the carbenium ion by 15 kJ mol^{-1} in the zeolite.

Thus, we conclude that sorbed cyclohexanol is bound primarily through dispersion forces and specifically adsorbed at Brønsted acid sites in protonated form. Under the present experimental conditions only approximately 5% of cyclohexanol in the pores is adsorbed in the latter form. Water elimination follows an E1 mechanism forming a cyclohexyl carbenium ion, which either undergoes rapid 1,2-hydride shift or is rehydrated, thus, scrambling the label in cyclohexanol. Transfer of the proton back to HBEA closes the catalytic cycle and leads to the primary product, cyclohexene. Alternatively, the cyclohexyl oxonium ion reacts with another cyclohexanol forming dicyclohexyl ether, in analogy to dimethyl ether formation.[22] In approaching the equilibrium, the cyclohexyl carbenium ion also undergoes nucleophilic addition of cyclohexene leading to C–C coupling and formation of cyclohexyl-1-cyclohexene.

The results show that the novel microautoclave NMR rotor developed allows kinetic and mechanistic studies of solid–liquid–gas and liquid–liquid–gas reactions at high temperatures and pressures to an unprecedented extent. The breadth and depths of mechanistic studies will only be limited by the sensitivity of the NMR spectrometer to differentiate the isotopomers of the reacting species.

Experimental Section

NMR experiments were performed on a 500 MHz wide bore NMR spectrometer equipped with a homemade 9.5 mm MAS probe.[12e] A single pulse sequence with a 45-degree pulse angle and high-power proton decoupling was used. As example experiment: in situ ^{13}C MAS-NMR spectra were acquired as function of time while spinning the sample, a mixture of HBEA150 (22 mg) and 1-^{13}C-cyclohexanol (120 μL of 0.33 M) in water at estimated 130 °C, at 2.4 kHz. A recycle delay of 5 s and an accumulation number of 256 scans was applied resulting in acquisition times for a single spectrum of approximately 0.29 h. The temperature in the microautoclave was calibrated prior to the experiment using $Pb(NO_3)_2$.[23] To minimize conversion of 1-^{13}C-cyclohexanol prior to a kinetic run, the temperature of the sample was raised to 130 °C in two steps, first to 80 °C, at which time spectrometer settings were checked, and then to the reaction temperature. The heat-up time for this second step was approximately 5 min. In this way less than 2% of 1-^{13}C-cyclohexanol was converted prior to acquiring the first spectrum in Figure 2 (see the Supporting Information for details). To assure quantitative analysis of obtained ^{13}C NMR spectra $T1$ values for cyclohexanol and cyclohexene were measured at RT and reaction temperature. Results are available in the Supporting Information. HBEA150 (Si/Al = 75) was obtained from Süd Chemie AG (Clariant) in hydrogen form (see the Supporting Information). As an example of the batch autoclave experiment: HBEA150 (17.4 g) and cyclohexanol (80 mL of 0.33 M) in water were placed in the 300 mL Hastelloy Parr reactor, heated to 160 °C, and stirred vigorously as temperature setting is reached. After a set time, the reactor was cooled with ice, leading to a rapid cool down and reaction quench. Contents of the reactor were extracted with

dichloromethane and dried with sodium sulfate. The extract was analyzed on an Agilent 7890 A GC equipped with a HP-5MS 25 m 0.25 μm inner diameter column, coupled with an Agilent 5975C MS.

Periodic density functional calculations (DFT) were performed using the CP2K code.[24] Calculations employ a mixed Gaussian and plane wave basis sets. Core electrons were represented with norm-conserving Goedecker–Teter–Hutter pseudopotentials[25] and the valence electron wave function was expanded in a double-zeta basis set with polarization functions[26] along with an auxiliary plane wave basis set with an energy cutoff of 360 eV. The generalized gradient approximation exchange-correlation functional of Perdew, Burke, and Enzerhof (PBE)[27] was used for all calculations. Each configuration was optimized with Broyden–Fletcher–Goldfarb–Shanno (BGFS) algorithm with SCF convergence criteria of 10^{-8} au. To compensate long-range van der Waals (VdW) interaction between adsorbate and zeolite, DFT-D3 scheme[28] with an empirical damped potential term was added into the energies obtained from exchange-correlation functional. Transition states for protonation, configuration transformation, and dehydration steps in HBEA pore were located using the IT-NEB method[29] with seven images between initial and final state.

Received: July 31, 2013
Revised: October 8, 2013
Published online: November 26, 2013

Keywords: alcohol dehydration · heterogeneous catalysis · NMR spectroscopy · reaction mechanisms · zeolites

[1] D.-Y. Hong, S. J. Miller, P. K. Agrawal, C. W. Jones, *Chem. Commun.* **2010**, *46*, 1038 – 1040.
[2] C. Zhao, J. He, A. A. Lemonidou, X. Li, J. A. Lercher, *J. Catal.* **2011**, *280*, 8 – 16.
[3] C. Zhao, S. Kasakov, J. He, J. A. Lercher, *J. Catal.* **2012**, *296*, 12 – 23.
[4] C. Zhao, J. A. Lercher, *ChemCatChem* **2012**, *4*, 64.
[5] C. Zhao, D. M. Camaioni, J. A. Lercher, *J. Catal.* **2012**, *288*, 92 – 103; C. Zhao, W. Song, J. A. Lercher, *ACS Catal.* **2012**, *2*, 2714 – 2723.
[6] a) E. G. Derouane, *J. Catal.* **1986**, *100*, 541; b) E. Kikuchi, H. Nahano, K. Shinomura, Y. Morita, *Sekiyu Gakkaishi* **1985**, *28*, 210.
[7] M. Brändle, J. Sauer, *J. Am. Chem. Soc.* **1998**, *120*, 1556 – 1570.
[8] F. Carey, R. Sundberg, *Advanced Organic Chemistry*, Springer, New York, **2007**, pp. 473 – 577.
[9] M. Janik, J. Macht, E. Inglesia, M. Neurock, *J. Phys. Chem. C* **2009**, *113*, 1872 – 1885.
[10] A. Corma, H. Garcia, *Catal. Today* **1997**, *38*, 257 – 308.
[11] D. E. Bryant, W. L. Kranich, *J. Catal.* **1967**, *8*, 8 – 13.
[12] a) J. F. Haw, B. R. Richardson, I. S. Oshiro, N. D. Lazo, J. A. Speed, *J. Am. Chem. Soc.* **1989**, *111*, 2052 – 2058; b) W. Wang, J. Jiao, Y. Jiang, S. S. Ray, M. Hunger, *ChemPhysChem* **2005**, *6*, 1467 – 1469; c) J. Z. Hu, J. A. Sears, H. S. Mehta, J. J. Ford, J. H. Kwak, K. Zhu, Y. Wang, J. Liu, D. W. Hoyt, C. H. F. Peden, *Phys. Chem. Chem. Phys.* **2012**, *14*, 2137 – 2143; d) A. Aerts, C. E. A. Kirschhock, J. A. Martens, *Chem. Soc. Rev.* **2010**, *39*, 4626 – 4642; e) H. Ernst, D. Freude, T. Mildner, I. Wolf, *Solid State Nucl. Magn. Reson.* **1996**, *6*, 147 – 156.
[13] a) F. Taulelle, M. Haouas, C. Gerardin, C. Estourned, T. Loiseau, G. Ferey, *Colloids Surf. A* **1999**, *158*, 299 – 311; b) O. B. Vistad, D. E. Akporiaye, F. Taulelle, K. P. Lillerud, *Chem. Mater.* **2003**, *15*, 1639 – 1649.
[14] F. Zaera, *Chem. Rev.* **2012**, *112*, 2920 – 2986.
[15] a) D. W. Hoyt, R. V. F. Turcu, J. A. Sears, K. M. Rosso, S. D. Burton, A. R. Felmy, J. Z. Hu, *J. Magn. Reson.* **2011**, *212*, 378 – 385; b) R. V. F. Turcu, D. W. Hoyt, K. M. Rosso, J. A. Sears, J. S. Loring, A. R. Felmy, J. Z. Hu, *J. Magn. Reson.* **2013**, *226*, 64 – 69.
[16] a) F. Eder, M. Stockenhuber, J. A. Lercher, *J. Phys. Chem. B* **1997**, *101*, 5414; b) B. de Moor, M. F. Reyniers, J. A. Lercher, G. Marin, *J. Phys. Chem. C* **2011**, *115*, 1204.
[17] T. S. Sorensen, S. M. Whitworth, *J. Am. Chem. Soc.* **1990**, *112*, 6647 – 6651.
[18] a) P. A. Jacobs, M. Tielen, J. B. Uytterhoeven, *J. Catal.* **1977**, *50*, 98 – 108; b) S. J. Gentry, R. Rudham, *J. Chem. Soc. Faraday Trans. 1* **1974**, *70*, 1685 – 1692.
[19] H. Chiang, A. Bhan, *J. Catal.* **2010**, *271*, 251 – 261.
[20] B. Hunger, S. Matysik, M. Heuchel, W. D. Einicke, *J. Therm. Anal. Calorim.* **2001**, *64*, 1183 – 1190.
[21] T. Maihom, P. Khongpracha, J. Sirijaraensre, J. Limtrakul, *ChemPhysChem* **2013**, *14*, 101 – 107.
[22] a) S. R. Blaszkowski, R. A. van Santen, *J. Am. Chem. Soc.* **1996**, *118*, 5152 – 5153; b) S. Namuangruk, J. Meeprasert, P. Khemthong, K. Faungnawakij, *J. Phys. Chem. C* **2011**, *115*, 11649 – 11656; c) X. Liang, A. Montoya, B. S. Haynes, *J. Phys. Chem. B* **2011**, *115*, 8199 – 8206.
[23] T. Takahashi, H. Kawashima, H. Sugisawa, T. Baba, *Solid State Nucl. Magn. Reson.* **1999**, *15*, 119 – 123.
[24] CP2K Open Source Molecular Dynamics Program, http://www.cp2k.org/.
[25] a) S. Goedecker, M. Teter, J. Hutter, *Phys. Rev. B* **1996**, *54*, 1703; b) C. Hartwigsen, S. Goedecker, J. Hutter, *Phys. Rev. B* **1998**, *58*, 3641; c) M. Krack, *Theor. Chem. Acc.* **2005**, *114*, 145.
[26] J. VandeVondele, J. Hutter, *J. Chem. Phys.* **2007**, *127*, 114105.
[27] J. P. Perdew, K. Burke, M. Ernzerhof, *Phys. Rev. Lett.* **1996**, *77*, 3865.
[28] S. Grimme, J. Antony, S. Ehrlich, H. Krieg, *J. Chem. Phys.* **2010**, *132*, 154104.
[29] a) G. Henkelman, B. P. Uberuaga, H. Jonsson, *J. Chem. Phys.* **2000**, *113*, 9901; b) G. Mills, H. Jonsson, G. K. Schenter, *Surf. Sci.* **1995**, *324*, 305.

